Electronic supplementary information (ESI)

Synthesis of Gallic Acid Grafted Epoxidized Natural Rubber and its Role in Self-Healable Flexible Temperature Sensor

Aparna Guchait, Simran Sharma, Santanu Chattopadhyay*, Titash Mondal*

Rubber Technology Centre, Indian Institute of Technology Kharagpur, Kharagpur, India-721302

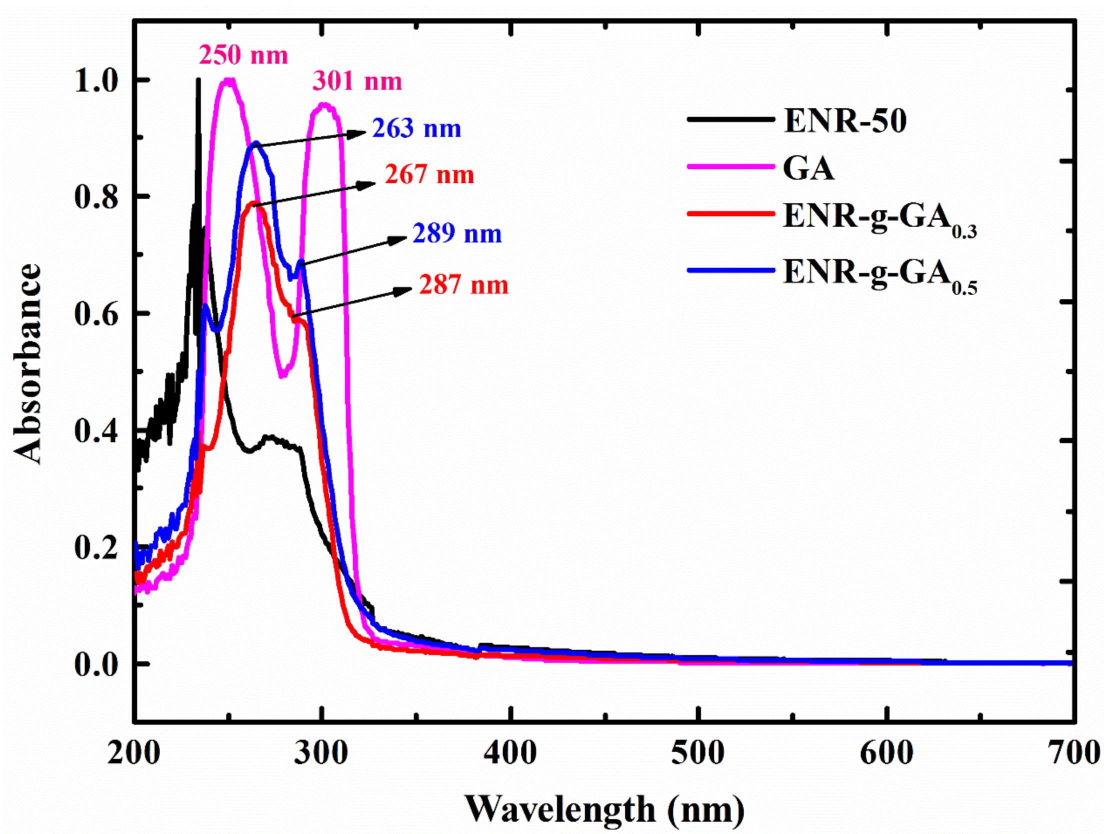

Fig. S1: UV-vis spectra of unmodified ENR-50, GA, and ENR-g-GA.

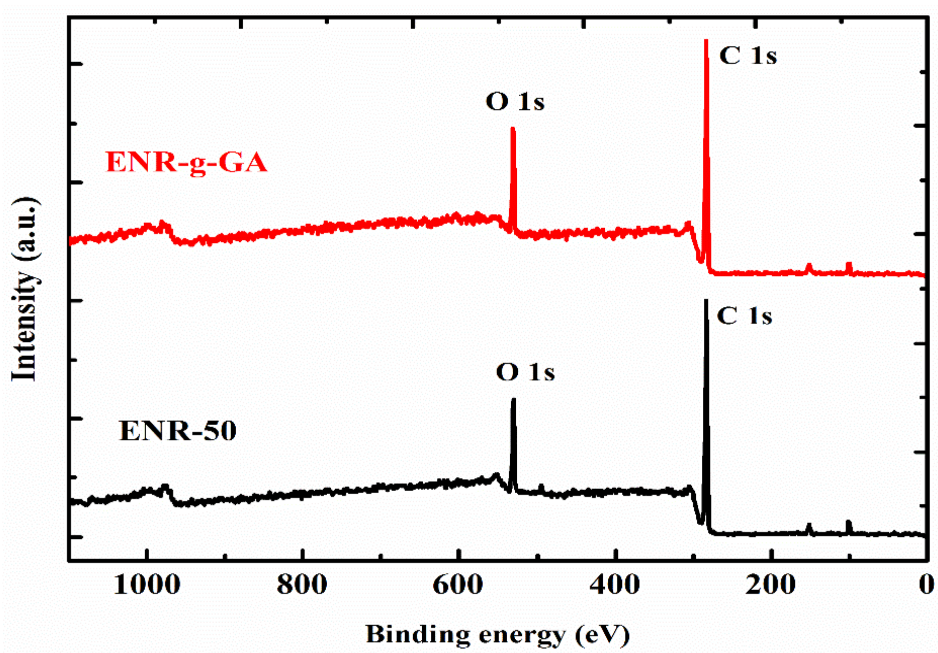

Fig. S2: XPS survey scan of pristine ENR-50 and ENR-g-GA

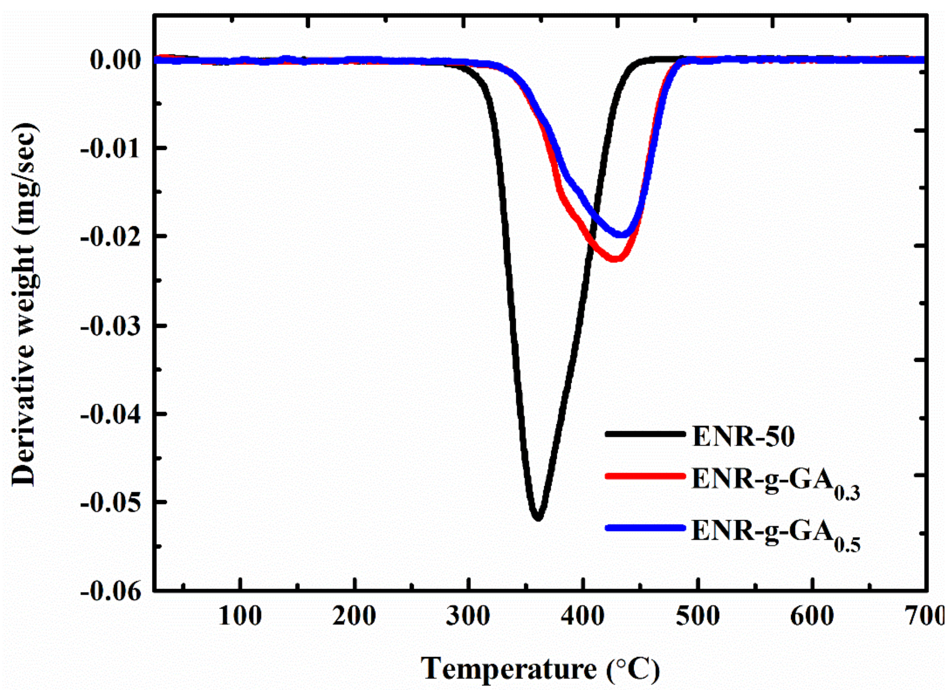

Fig. S3: DTG thermogram of ENR-50 and ENR-g-GA.

Table S1: Thermal degradation of ENR, ENR-g-$GA_{0.3}$, ENR-g-$GA_{0.5}$

Sample Name	T_{10} (ºC)	T_{50} (ºC)	T_{90} (ºC)	Residue (%)
ENR-50	336	367	407	1.9
ENR-g-$GA_{0.3}$	365	414	451	0.3
ENR-g-$GA_{0.5}$	365	417	454	0.2

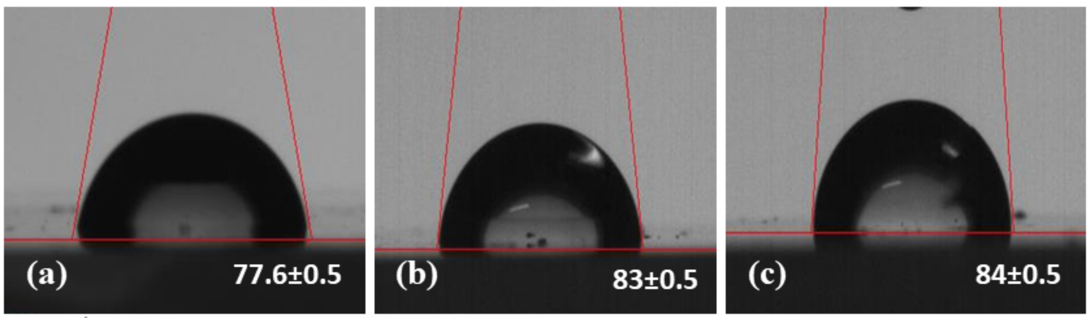

Fig. S4: Contact angle of pristine ENR-50 (a), ENR-g-$GA_{0.3}$ (b) and ENR-g-$GA_{0.5}$ (c)

Table S2: Contact angle and work of adhesion value for pristine ENR-50, ENR-g-$GA_{0.3}$ and ENR-g-$GA_{0.5}$

Parameter	Purified ENR-50	ENR-g-$GA_{0.3}$	ENR-g-$GA_{0.5}$
Contact angle (º)	77.6 ± 0.5	83 ± 0.5	84 ± 0.5
W_{SL}(J/m²)	88.36	80.7	79.5

Table S3: Tensile strength and elongation value of the sample.

Sample name	Tensile strength (MPa)	Elongation at Break (%)
ENR/$Fe^{3+}_{0.02}$	2.73 ± 0.25	748 ± 37
ENR-g-GA/$Fe^{3+}_{0.02}$	4.42 ± 0.13	667 ± 25
ENR/$Fe^{3+}_{0.05}$	3.71 ± 0.05	561 ± 97
ENR-g-GA/$Fe^{3+}_{0.05}$	6.5 ± 0.34	451 ± 54
ENR/$Fe^{3+}_{0.10}$	5.1 ± 0.23	470 ± 59
ENR-g-GA/$Fe^{3+}_{0.10}$	19.6 ± 0.33	248 ± 13
ENR/$Fe^{3+}_{0.15}$	8.5 ± 0.85	429 ± 13
ENR-g-GA/$Fe^{3+}_{0.15}$	14.8 ± 0.58	12 ± 2.2

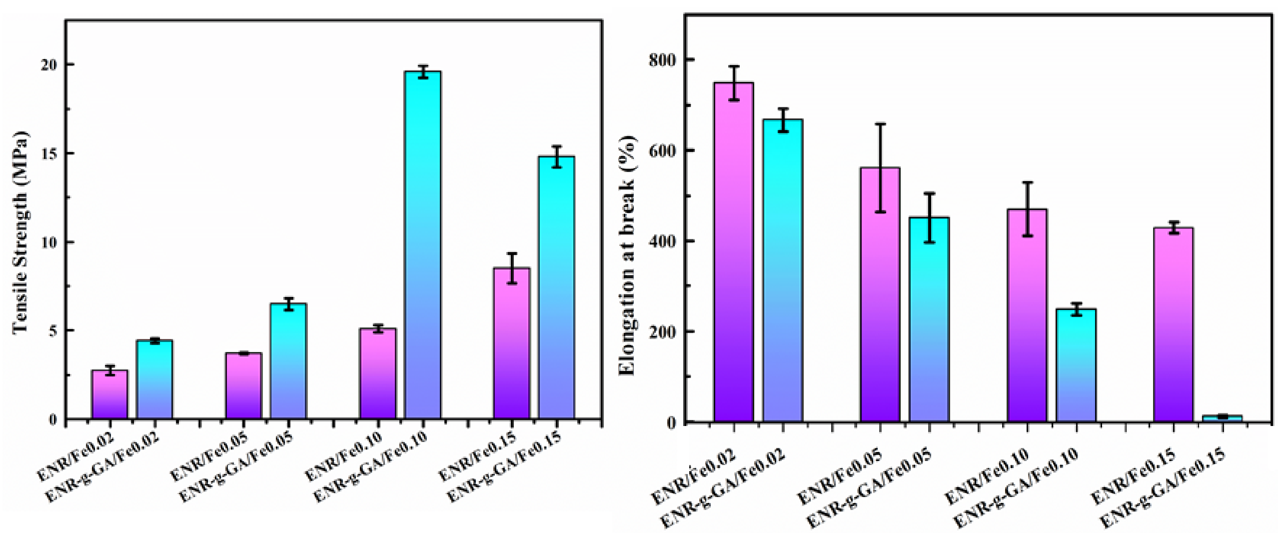

Fig. S5: Tensile strength and elongation at break.

Table S4: Tensile strength of ENR-g-GA/Fe with different Fe^{3+} content and CNT filled ENR-g-GA/Fe with different CNT loading.

Sample	Tensile strength (MPa)	EAB	Efficiency of tensile strength	Efficiency of EAB
ENR-g-GA/$Fe^{3+}_{0.02}$	4.42	667		
ENR-g-GA/$Fe^{3+}_{0.02}$**H**	1.90	323	42.9%	48.4%
ENR-g-GA/$Fe^{3+}_{0.05}$	6.5	451		
ENR-g-GA/$Fe^{3+}_{0.05}$**H**	1.57	118	24.1%	26.1%
ENR-g-GA/$Fe^{3+}_{0.10}$	19.59	248		
ENR-g-GA/$Fe^{3+}_{0.10}$**H**	1.33	87	6.7%	35%
ENR-g-GAC2/$Fe^{3+}_{0.02}$	3.2	617		
ENR-g-GAC2/$Fe^{3+}_{0.02}$**H**	1.0	146	31.2%	23.6%

Table S5: Temperature sweep

	Temperature (º C)	**Tan delta**
ENR/$Fe^{3+}_{0.10}$	-4.5	0.508
ENR-g-GA/$Fe^{3+}_{0.02}$	11.75	1.27
ENR-g-GA/$Fe^{3+}_{0.05}$	14.99	0.687
ENR-g-GA/$Fe^{3+}_{0.15}$	20.8	0.583

Table S6: Frequency sweep

	Log frequency	**Log E', E"**
ENR/$Fe^{3+}_{0.10}$	-1.85	6.12
ENR-g-GA/$Fe^{3+}_{0.05}$	-1.64	6.257
ENR-g-GA/$Fe^{3+}_{0.10}$	-1.44	6.287

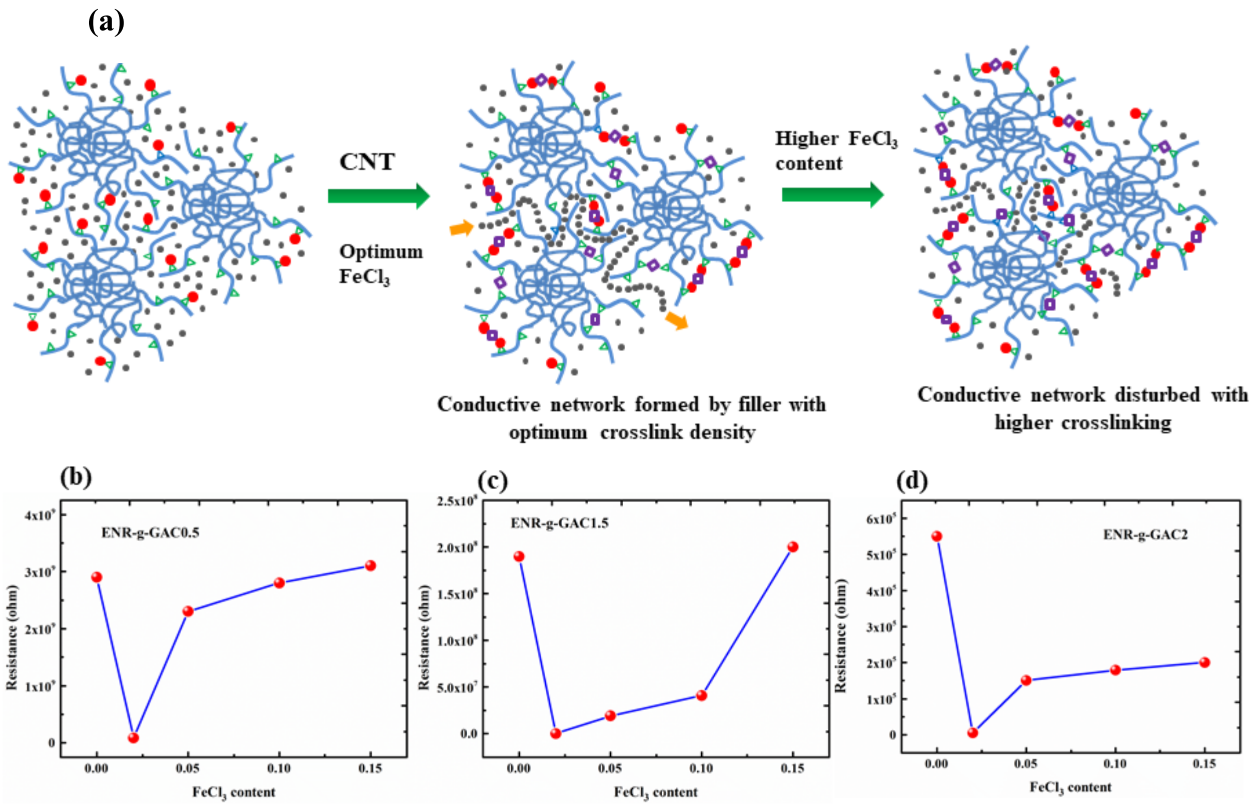

Fig. S6: (a) Schematic representation of effect of conductivity with $FeCl_3$ content. Resistance vs $FeCl_3$ content for ENR-g-GAC0.5 (CNT content 0.5%) (b), ENR-g-GAC1.5 (CNT content 1.5%) (c), ENR-g-GAC2 (CNT content 2%) (e).

Figure S6a demonstrated the schematic diagram of effect of crosslink (with respect to $FeCl_3$ content) on the conductivity. Figure S6(b-d) represent the resistance value of the composite film with varying $FeCl_3$ content for CNT loading of 0.5%, 1.5%, 2%. All this figure showed a decrease in resistance for $FeCl_3$ 0.02, then increases with increasing amount of $FeCl_3$. This can be explained by the fact that, at an optimum $FeCl_3$ content, the conductive filler particles are forced to come in a close proximity. Therefore, a small amount of $FeCl_3$ form a conductive filler network which reduced the resistance of the composite film. However, with increasing $FeCl_3$ content the filler particles are bound in small area due to the increase in crosslink density, which imparts disconnect in the filler network. Therefore, with increasing $FeCl_3$ beyond an optimal value the resistance value increases.

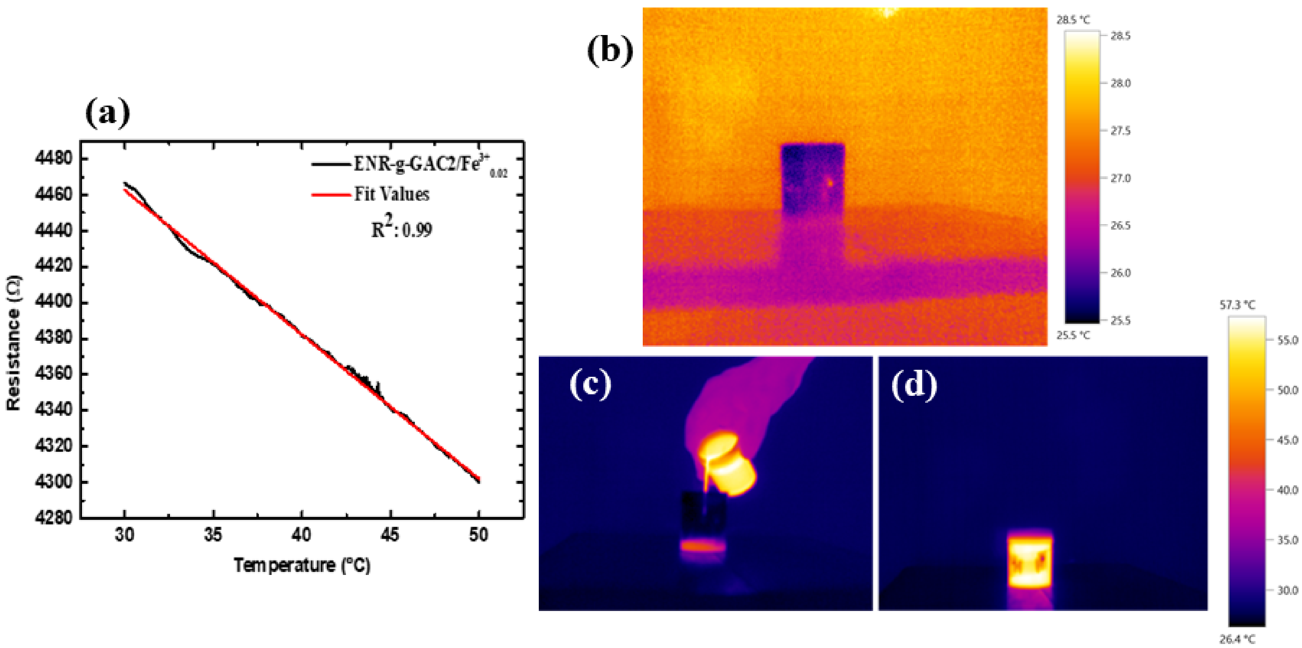

Fig. S7: (a) resistance vs temperature plot, (b-d) thermal camera image

Table S7: Tensile strength of the sensor and the healed sensor sample.

Sample	Tensile strength (MPa)	EAB	Efficiency of tensile strength	Efficiency of EAB
ENR-g-GAC2/$Fe^{3+}_{0.02}$	3.2	617		
ENR-g-GAC2/$Fe^{3+}_{0.02}$H	1.0	146	31.2%	23.6%